PASJ: Publ. Astron. Soc. Japan **52**, 955–965 (2000)

The VLBI Space Observatory Programme and the Radio-Astronomical Satellite HALCA

Hisashi HIRABAYASHI,[1] Haruto HIROSAWA,[1] Hideyuki KOBAYASHI,[2] Yasuhiro MURATA,[1]
Yoshiharu ASAKI,[1] Ian M. AVRUCH,[1] Philip G. EDWARDS,[1] Edward B. FOMALONT,[1,6]
Tsutomu ICHIKAWA,[1] Tsuneo KII,[1] Rikako OKAYASU,[1,3,16] Kiyoaki WAJIMA,[1] Makoto INOUE,[2]
Noriyuki KAWAGUCHI,[2] Yoshihiro CHIKADA,[2] Takeshi BUSHIMATA,[2] Kenta FUJISAWA,[2]
Shinji HORIUCHI,[2] Seiji KAMENO,[2] Takeshi MIYAJI,[2] Kazunori M. SHIBATA,[2] Zhi-Qiang SHEN,[2]
Tomofumi UMEMOTO,[2] Takashi KASUGA,[3] Jun'ichi NAKAJIMA,[4] Yukio TAKAHASHI,[4]
Shinzou ENOME,[2] Masaki MORIMOTO,[2] Jordan ELLIS,[5] David L. MEIER,[5] David W. MURPHY,[5]
Robert A. PRESTON,[5] Joel G. SMITH,[5] Rick D. WIETFELDT,[5] John M. BENSON,[6]
Mark J. CLAUSSEN,[6] Chris FLATTERS,[6] George A. MOELLENBROCK,[6] Jonathan D. ROMNEY,[6]
James S. ULVESTAD,[6] Glen I. LANGSTON,[7] Anthony H. MINTER,[7] Larry R. D'ADDARIO,[8]
Peter E. DEWDNEY,[9] Sean M. DOUGHERTY,[9,11] David L. JAUNCEY,[10] James E. J. LOVELL,[10]
Steven J. TINGAY,[10] Anastasios K. TZIOUMIS,[10] A. Russell TAYLOR,[11] Wayne H. CANNON,[12]
Leonid I. GURVITS,[13] Richard T. SCHILIZZI,[13] Roy S. BOOTH,[14] Misha V. POPOV[15]

[1] *The Institute of Space and Astronautical Science, 3-1-1 Yoshinodai, Sagamihara, Kanagawa 229-8510*
[2] *National Astronomical Observatory, 2-21-1 Osawa, Mitaka, Tokyo 181-8588*
[3] *Department of System and Control Engineering, Hosei University, 3-7-2 Kajino-cho, Koganei-shi, Tokyo 184-8584*
[4] *Communications Research Laboratory, Hirai 893-1, Kashima, Ibaraki 314-0012*
[5] *Jet Propulsion Laboratory, 4800 Oak Grove Drive, Pasadena, CA 91109, USA*
[6] *National Radio Astronomy Observatory, P.O. Box 0, Socorro, NM 87801, USA*
[7] *National Radio Astronomy Observatory, P.O. Box 2, Green Bank, WV 24944, USA*
[8] *National Radio Astronomy Observatory, 949 N Cherry Ave, Tucson AZ 85721-0655, USA*
[9] *National Research Council of Canada, Herzberg Institute of Astrophysics, Dominion Radio Astrophysical Observatory, Penticton, British Columbia V2A 6K3, Canada*
[10] *Australia Telescope National Facility, P.O. Box 76, Epping, New South Wales 2122, Australia*
[11] *Physics and Astronomy Department, University of Calgary, 2500 University Dr. NW, Calgary, Alberta, T2N 1N4 Canada*
[12] *Center for Research in Earth and Space Technology/York University, 4850 Keele St., North York, Ontario, M3J 3K1 Canada*
[13] *Joint Institute for VLBI in Europe, Postbus 2, 7991 PD Dwingeloo, The Netherlands*
[14] *Onsala Space Observatory, Chalmers University of Technology, S-43992 Onsala, Sweden*
[15] *Astro Space Center, P.N. Lebedev Physical Institute, Profsoyuznaya 84/32, Moscow 117810, Russia*
[16] *Department of Engineering, Kanagawa University, 3-27-1 Rokkaku-bashi, Yokohama, Kanagawa 221-8686*

(Received 2000 July 7; accepted 2000 August 7)

Abstract

The radio astronomy satellite HALCA was launched by the Institute of Space and Astronautical Science in 1997 February to participate in Very Long Baseline Interferometry (VLBI) observations with arrays of ground radio telescopes. HALCA is the main element of the VLBI Space Observatory Programme (VSOP), a complex international endeavor involving over 25 ground radio telescopes, five tracking stations and three correlators. Simultaneous observations with HALCA's 8 meter diameter radio telescope and ground radio telescopes synthesize a radio telescope over twice the size of the Earth, enabling the highest resolution 1.6 GHz and 5 GHz images to be made.

Key word: space vehicles: instruments — techniques: interferometric — radio continuum: galaxies

1. Introduction

Very Long Baseline Interferometry (VLBI) is a powerful technique for high angular resolution radio imaging (see, e.g., the reviews by Schilizzi 1995; Zensus 1997). In VLBI observations, widely spaced radio telescopes simultaneously observe the same celestial radio source, digitize the radio signal, and record the data on magnetic tape. The tapes are later brought together at a correlator for the data to be combined (e.g., Thompson et al. 1986).

The longest baselines, D, obtainable in ground-based VLBI observations are $\sim$ 10000 km. Thus, for observations at 5 GHz (λ = 6 cm), the Earth-based resolution limit, λ/D, is about 1 milli-arcsecond (mas). However, many galactic and extragalactic radio sources contain components that remain unresolved with the highest angular resolution available using ground-based VLBI networks.

The idea of improving the resolution by having at least one element of a VLBI array on an Earth-orbiting spacecraft — 'space VLBI' — has been under discussion since soon after the first successful VLBI observations were made (see, e.g., Burke 1984). The feasibility of VLBI with an orbiting element was demonstrated in a series of experiments with a Tracking and Data Relay Satellite System (TDRSS) communications satellite. Observations using the 4.9 m antenna of a TDRSS satellite and 2–3 ground radio telescopes at 2.3 GHz and 15 GHz were made between 1986 and 1988, demonstrating that space VLBI is technically possible and that sources could be detected on baselines of up to two Earth diameters (Levy et al. 1986; Linfield et al. 1989, 1990). These observations together with studies for the RadioAstron (Kardashev, Slysh 1988), QUASAT (Schilizzi 1988), and IVS (Pilbratt 1991) missions paved the way for the development of the satellite MUSES-B (Hirosawa, Hirabayashi 1996) by the Institute of Space and Astronautical Science (ISAS). The primary goals of this satellite were to test the technologies required for VLBI in space, foremost of which is the deployable main reflector of the radio telescope, to develop stable two-way communications between the satellite and ground tracking stations, and to accurately determine the satellite's orbit. The satellite is the orbital element of the VLBI Space Observatory Programme (VSOP), which is a large international collaboration of space agencies and ground observatories which have combined resources to create the first dedicated space VLBI mission. An overview of the mission and several of the first images were presented in Hirabayashi et al. (1998); in this paper a more thorough technical description is given.

2. The HALCA Satellite

The MUSES-B satellite was launched on the first flight of ISAS's M-V rocket from the Kagoshima Space Center on 1997 February 12. At launch the satellite's mass was 830 kg, of which 62 kg was hydrazine used by the Reaction Control System (RCS) thrusters for perigee-raising maneuvers and safe-hold events. After the successful launch the satellite was renamed HALCA — an acronym for the Highly Advanced Laboratory for Communications and Astronomy. The solar paddles and boom-mounted 45 cm diameter link antenna were deployed during the satellite's first orbit. After three perigee-raising maneuvers, HALCA was placed in an orbit with an apogee height above the Earth's surface of 21400 km, a perigee height of 560 km, and an orbital period of 6.3 hr. The orbit thus enables imaging VLBI observations on baselines over three-times longer than those achievable on Earth. HALCA's orbital plane is inclined by $31\overset{\circ}{.}3$ to the Earth's equatorial plane and, due to gravitational torques induced by the oblateness of the Earth, precesses with time. The precession is described by the rates of change of the argument of perigee and the longitude of the ascending node, which have periods of about 1 yr and 1.6 yr, respectively. VSOP observations yield the maximum resolution for sources near the orbit normal directions, and the precession of the orbit means that good resolution can be obtained for a large region of the sky over the $\sim$ 5 yr lifetime of the mission.

HALCA's radio telescope, illustrated in figure 1, has a main reflector with an effective diameter of 8 m, consisting of a mesh of gold-coated molybdenum wire, suspended between six extendible masts and shaped by a tension-truss arrangement (Natori et al. 1993). It uses Cassegrain optics, with a hexagonal sub-reflector inscribed in a 1.1 m diameter circle. The sub-reflector was deployed on 1997 February 24 and placed 3.4 m above the surface of the main reflector. Deployment of the main antenna masts took place over 1997 February 26–27 (Natori et al. 1998).

The on-board radio-astronomy observing system is described in detail in a following paper (Kobayashi et al. 2000a). All frequencies on-board the satellite are locked to a tone derived from a hydrogen maser standard at one of five dedicated ground tracking stations and transmitted at 15.3 GHz to the 45 cm on-board link antenna. HALCA's radio astronomy receivers detect left-circularly polarized radiation, with observing frequency ranges 1.60–1.73 GHz, 4.7–5.0 GHz, and 22.0–22.3 GHz. Due to a large attenuation in the on-board system at 22 GHz scientific observations are carried out in the 1.6 GHz and 5.0 GHz bands; however, the successful detection of fringes to HALCA at 22 GHz confirms that all other mission elements perform well at this frequency (Kobayashi et al. 2000b). The standard observing mode

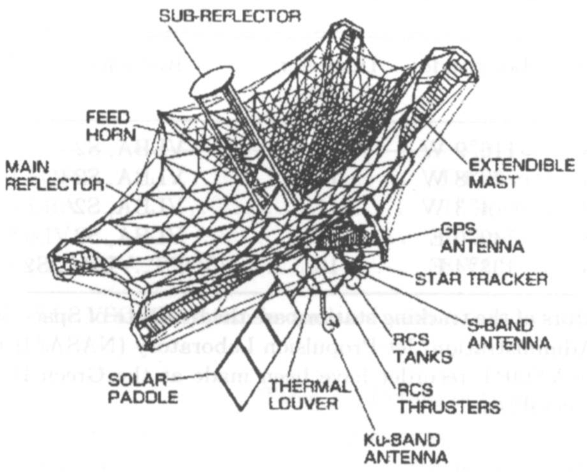

Fig. 1. Line drawing of the HALCA satellite after deployment in orbit of the main antenna (Hirosawa, Hirabayashi 1995). The two solar paddles, each with three panels of solar cells, cover a total area of 7 m^2. The Reaction Control System (RCS) thrusters were used in perigee raising maneuvers, but are not used in normal day-to-day operations. The satellite has one 14.2–15.3 GHz and three 2.1–2.3 GHz antennas, both bands being used for two-way communications.

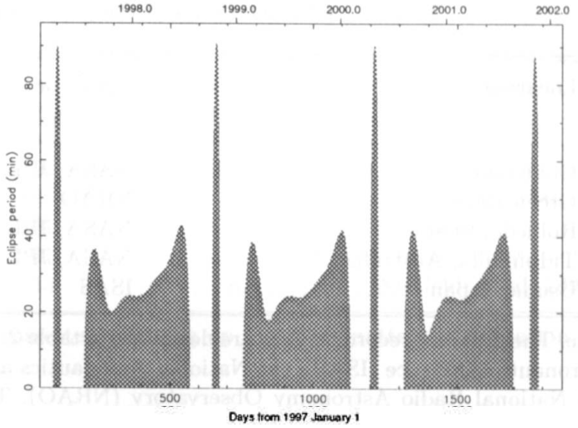

Fig. 2. Duration of eclipses of the Sun by the Earth, as seen from HALCA, as a function of time. Observing is not possible during an eclipse, nor during a similar length of time after the eclipse while the batteries fully recharge. No observing is carried out during the short periods of long (up to 90 min) eclipses.

uses two 16 MHz base-band channels, each digitized at 32 mega-samples per second with two bits per sample, generating data at 128 mega-bits per second. VLBI data is transmitted to the ground in real-time at 14.2 GHz via the 45 cm link antenna.

Two-way telemetry between the satellite and the 20 m antenna of the Kagoshima Space Center is used six days per week for commanding of the spacecraft at 2.1 GHz and down-linking on-board status information at 2.3 GHz. Commands for the next day or two are uplinked during the commanding sessions and then executed autonomously by the spacecraft.

The gain of HALCA's radio telescope has been determined by measuring the increase in detected power during five-point cross-scan observations of Cygnus A, yielding values of 0.0043 K Jy^{-1} at 1.6 GHz and 0.0062 K Jy^{-1} at 5 GHz. These correspond to efficiencies of 24% at 1.6 GHz and 35% at 5 GHz. The system temperature of the HALCA radio telescope is determined by comparing the signal levels measured with a noise diode switched on and off (Kobayashi et al. 2000a). Typical values are 75 K at 1.6 GHz and 95 K at 5 GHz (Moellenbrock et al. 2000). These system temperatures are combined with the gain to give system equivalent flux densities (SEFDs) of 17400 Jy at 1.6 GHz and 15300 Jy at 5 GHz with uncertainties in these values of $\sim 10\%$.

The satellite has two solar paddles with a total area of 7 m^2 to supply power. About 700 W was being generated after one year in orbit, with the solar panel efficiency decreasing with time due to degradation caused by cosmic radiation. Two Ni–Cd batteries are used as back-up power supplies and to power the satellite during eclipses.

Pointing of the spacecraft and its large telescope is carried out by reaction wheels, which apply torque to the spacecraft to rotate it in the desired direction (Ninomiya et al. 1991). Four reaction wheels were used, allowing zero-momentum attitude control, until 1999 October, after which the satellite has been operated in a three reaction wheel (biased momentum) mode (Murata et al. 2000). Maneuvers are performed in two stages, with a first slew around the satellite–Sun axis followed by a slew about the solar-paddle axis. The maximum slew rate is $2.^\circ25$ per minute. Mechanical gyroscopes are used to measure the angular motions while slewing. After the maneuver has been completed, two star trackers, mounted on opposite sides of the spacecraft, are used to check the pointing and to calibrate the gyroscopes. The angular momentum accumulated by the reaction wheels is dumped by magnetic torquers during perigee passes, using the Earth's magnetic field.

Observing is constrained by a number of conditions. HALCA cannot observe if the Sun angle, defined as the angle between the Sun and the source being observed, is less than 70° as the main antenna shadows the solar panels at these angles. Observations have been further limited to Sun angle ranges of typically 80–110° and 145–180° due to excessive angular momentum build-up experienced at intermediate angles. No observing is possible when the Sun is eclipsed by the Earth or Moon. As shown in figure 2, the precession of HALCA's orbit and

Table 1. Characteristics of the phase transfer and VLBI data acquisition tracking stations.

Location	Operator	Latitude	Longitude	Diameter (m)	Recorders
Goldstone, USA	NASA/JPL	35°3 N	116°9 W	11	VLBA, S2
Green Bank, USA	NRAO	38°4 N	79°8 W	14	VLBA, S2
Robledo, Spain	NASA/JPL	40°4 N	4°3 W	11	VLBA, S2
Tidbinbilla, Australia	NASA/JPL	35°4 S	149°0 E	11	VLBA, S2
Usuda, Japan	ISAS	36°1 N	138°4 E	10	VSOPT, VLBA, S2

Note. The different recorder types are described in table 2. The operators of the tracking stations are the Institute of Space and Astronautical Science (ISAS), the National Aeronautics and Space Administration/Jet Propulsion Laboratory (NASA/JPL), and National Radio Astronomy Observatory (NRAO). Tests with a VSOPT recorder have been made at the Green Bank tracking station, though this sytem has yet to be used for VSOP observations.

the Earth's motion around the sun result in two distinct eclipse cycles: a period of about one month when eclipses occur near apogee and are up to 90 min long each orbit, and a period of about a year when eclipses occur near perigee and are mostly 20–40 min long. A similar length of time to the eclipse duration is required to recharge the batteries before observing can recommence. To date, no observations have been conducted during the periods of long eclipses. In addition to these constraints, the 45 cm link antenna must be able to point at one of the five tracking stations.

3. Tracking Stations

The basic characteristics of the five dedicated tracking stations are described in table 1. A two-way link between the satellite and a ground tracking station is required for observing: the tracking station transmits the reference signal derived from its hydrogen maser, and receives and records the digitized astronomical signal from the satellite (D'Addario 1991a, b; Ulvestad 1999). For some part of each orbit no tracking station is visible. On average, the fraction of an orbit for which tracking is available ranges from 0.55 (when apogee is at its southernmost) to 0.85 (when apogee is at its northernmost).

All timing signals on the spacecraft, including local oscillators and data-sampling clocks, are phase-locked to the reference signal transmitted by a ground tracking station. For HALCA, the frequency of the up-link reference tone must be very close to 15.3 GHz, as received at the spacecraft in its local reference frame. Due to the motion of the satellite with respect to the tracking station, the uplink phase is varied with time to compensate for the predicted Doppler effect.

A transponder aboard HALCA generates a tone at a frequency of exactly 142/153 times that of the received uplink, or 14.2 GHz nominally. This is the carrier for the downlink transmission of the astronomical signal, as discussed below. At the tracking station, the carrier is extracted from the received downlink signal and its phase is measured with respect to that of a *predicted* downlink carrier synthesized at the station. The latter is based on the predicted orbital motion. Care is taken to track variations in this *residual phase* over the tracking pass (which lasts up to several hours), so that changes of many times 2π are measured without cycle slips. From the residual phase function, the timing error on the spacecraft can be derived, except for a fixed offset of an integer number of cycles of the downlink carrier (D'Addario 1991a, 1995).

If the predicted orbit were perfect and if delays introduced by the troposphere and ionosphere were exactly predictable, and if the equipment operated ideally, then no timing error would occur. Because such imperfections do exist, a variable timing error occurs on the spacecraft, but its value is accurately tracked by the residual phase measurements. The derived timing error function is used as a correction during the later correlation of the astronomical signals from the space and ground telescopes (see section 6). The unknown, integer-cycle offset in the timing error is no larger than the range component of the error in the orbit, typically about 50 ns (see section 4). Most critically, the continuous phase tracking means that the offset remains constant during the tracking pass; time-variable components of the error are removed to very high precision by the corrections (post-correction residuals are estimated to be constant to around 1 ps), thereby avoiding any significant de-correlation of the astronomical signals and limiting the amount of delay-offset searching required at correlation.

The Usuda tracking station can operate in a "closed loop" mode with the variable timing error corrected in real time (Suzuki et al. 2000). In this mode the constant offsets between the station clock and GPS and the fixed offset due to the error in the orbit at the initialization epoch are the only time corrections required. A minor disadvantage of this mode is that some data is lost at the start of the tracking pass while the feedback loop iterates

Table 2. Data recording systems used for VSOP observations.

Name	Type	Data capacity (giga-bytes)	Recording time at 128 mega-bit s^{-1} (hr)	Reference
VSOPT	D1 cassette	115	2.0	Iguchi et al. 2000
VLBA	1″ open reel tape	591	10.3	Rogers 1995
MkIV	1″ open reel tape	591	10.3	Whitney 1999
S2	8 VHS cassettes	345	6.0	Wietfeldt et al. 1996

Note. The VSOPT system is operated with a cart holding up to 24 cassettes, allowing up to 48 hr unattended operation.

Table 3. Details of the three correlators used for VSOP observations.

Correlator	Format	Number of station inputs	Maximum delay range (μs)	Maxiumum fringe-rate range (Hz)	Maximum number of spectral points per IF channel	Reference
Mitaka, Japan	VSOPT	10	± 256	± 40.0	8192	Chikada et al. 1991
Socorro, USA	VLBA/MkIV	20	± 32	± 3.9	1024	Benson 1995
Penticton, Canada	S2	6	± 256	± 250.0	8192	Carlson et al. 1999

Note. The full ranges cannot all be used at the same time: the correlation parameters must be selected so as not to exceed the maximum allowed correlator output rate.

to the correct value of the timing error. Furthermore, the loop bandwidth is limited by the round-trip time; faster fluctuations and/or higher orbits can be handled by the open loop correction method.

The 14.2 GHz transponder output is also used to carry the astronomical signal, which is digitized on the spacecraft. QPSK modulation is used at a clock rate of 64 MHz to transmit the 128 mega-bit per second data stream. Every 5 ms, 96 bits of signal data (0.015%) are replaced with a 32-bit synchronization code and 64 bits of housekeeping telemetry. At the tracking station, the signal is demodulated, the synchronization bits detected and telemetry extracted, and the signal bits are formatted for recording onto high-speed magnetic tape. Three different recording systems are in use at the tracking stations (table 1), and a fourth at some ground telescopes; major parameters of the four systems are listed in table 2.

4. Orbit Determination

Accurate knowledge of the satellite's predicted orbit is required in advance in order for the reference phase to be suitably offset at the tracking station before transmission to match the calculated Doppler shift of the satellite. Higher precision post-observation orbit solutions are required, as discussed below, in order to align in the correlator the data-streams from HALCA and the participating ground radio telescopes. These 'predicted' and 'reconstructed' orbit solutions are determined independently by navigation teams at ISAS and the Jet Propulsion Laboratory. The orbit determinations are based on range-rate data derived from the residual phase measurements conducted at 15 GHz by the five tracking stations, and from the range data calculated from 2 GHz tracking at the Kagoshima Space Center and NASA's Deep Space Network stations.

Uncertainties in the modelling of atmospheric drag near perigee and solar pressure forces on the spacecraft and telescope are the leading causes of errors in the reconstruction of the spacecraft orbit. Results to date indicate that the relative root-sum-of-squares errors in the JPL reconstructed orbits are 15 m in position — a result confirmed by a phase-referencing VSOP observation (Porcas et al. 2000) — and 6 mm s^{-1} in velocity (You et al. 1998). Differences in the models used by the orbit determination teams result in the ISAS reconstructed orbits having errors several times larger; however, these uncertainties can be dealt with by the wider search windows available at the Mitaka correlator (see table 3).

An accurate orbit determination requires 15 GHz range-rate data over a range of orbital phases, a need which is met during observations by regular switching between tracking stations to track the satellite around as much of the orbit as possible. During periods when no

Table 4. Participating ground radio telescopes.

GRT/Network	Location	Diameter (m)	SEFD (Jy) 1.6 GHz	SEFD (Jy) 5 GHz	Recorder
Arecibo	Puerto Rico	225	2.5	3.5	S2
ATCA	Australia	6 × 22	60	80	S2
Bear Lakes	Russia	64	100	—	S2
Ceduna	Australia	30	—	500	S2
Cambridge	UK	32	212	136	VLBA, MkIV
Effelsberg	Germany	100	19	20	VLBA, MkIV
Goldstone	USA	70	49	—	MkIV
Green Bank	USA	43	80	120	VLBA, S2
Hartebeesthoek	South Africa	26	370	680	S2, MkIV
Hobart	Australia	26	1300	1300	S2
Jodrell Bank (Lovell)	UK	76	44	—	VLBA, MkIV
Jodrell Bank (Mk II)	UK	26	—	320	VLBA, MkIV
Kalyazin	Russia	64	—	100	S2
Kashima	Japan	34	231	365	VSOPT
Medicina	Italy	32	582	296	MkIV
Mopra	Australia	22	350	450	S2
Noto	Italy	32	784	260	VLBA, S2
Onsala	Sweden	25	390	600	MkIV
Robledo	Spain	70	49	—	MkIV
Shanghai	China	25	1088	520	VLBA, S2
Tidbinbilla	Australia	70	49	—	MkIV, S2
Torun	Poland	32	200	220	VLBA
Usuda	Japan	64	69	69	VSOPT, S2, VLBA
VLA	USA	27 × 25	14	14	VLBA
VLBA	USA	10 × 25	300	290	VLBA
Westerbork	Netherlands	25	250	650	MkIV

Note. The system equivalent flux density (SEFD) listed for the VLBA (Very Long Baseline Array) is for a single antenna: for the VLA (Very Large Array) and ATCA (Australia Telescope Compact Array) it is for the full phased array. The Westerbork array has been refurbished during the first three years of the mission and the SEFD is for a single antenna, although VSOP observations with the full array of 14 antennas are envisaged in the future.

VSOP observing is being conducted, the tracking stations are regularly used to track HALCA for orbit determination purposes.

5. Ground Radio Telescopes

VSOP observations require the participation of a number of ground radio telescopes. Telescopes from the Very Long Baseline Array (Napier et al. 1994), the European VLBI Network (Schilizzi 1995), the Asia–Pacific Telescope (Tzioumis 1994) and other unaffiliated telescopes are combined to form ground arrays depending on the source position and the requirements of the observation. The properties of telescopes that have participated to date in VSOP observations are summarized in table 4. [In addition, the Kagoshima, Metsahovi, Mizusawa, Nobeyama, and Onsala (20 m) telescopes have participated in 22 GHz test observations.] The contributions of ground radio telescope time to the VSOP mission have been negotiated through the Global VLBI Working Group of URSI (the International Radio Science Union) Commission J on Radio Astronomy. Data are recorded at the telescopes in one of the four formats listed in table 2. For mixed-format observations, data can be translated at the Mitaka correlator and Usuda Tracking Station to the format appropriate for the correlator of that experiment (see table 3). Translation is possible between VSOPT and S2 formats, and VSOPT and VLBA formats: translation between S2 and VLBA formats is thus a two-stage process. Translation to and from MkIV format is not possible. A VSOPT terminal and S2 playback terminal have recently been added to the Green Bank tracking station, which may also enable data translation at this site.

6. Correlation

VLBI data from each observatory are brought together after the observation at a correlator. Ideally, during correlation the geometrical delays and timing errors for each interferometer element, and their rate of change with time, are corrected so that the data from all telescopes are synchronized; however, this is not exactly achievable in practice. Correlation proceeds by correcting for the delay and 'delay-rate' (first time derivative of the delay) as much as possible, and then cross-correlating the data recorded at each pair of telescopes with a range of values chosen to encompass the actual delay and delay-rate. The actual values of the delay and delay-rate are then determined during post-correlation analysis.

The location of telescopes on the Earth's surface is typically known with centimeter-level accuracy, and the orientation of the Earth with respect to the celestial sphere is also accurately known. Each observatory uses a high-accuracy hydrogen maser as a frequency standard, with the offset between the station time and time obtained from a fleet of Global Positioning System (GPS) satellites measured regularly. As a result, the relative time error between any two ground telescopes can be known with an accuracy of better than 100 ns.

For ground-only VLBI observations, the dominant uncertainties in the delay model at the correlators are the sampling time errors, typically 100 ns or less, and errors in the delay rate, of typically $\sim 10^{-14}$, caused by drifts in the maser clock and by atmospheric propagation along the line of sight to the source.

Space VLBI is considerably more complex than ground VLBI, as HALCA's reference phase originates from, and VLBI data is recorded at, a tracking station that may be over 25000 km from the satellite. Two additional sets of information are required by a correlator to handle VSOP data. the reconstructed orbit and the time correction series.

The accuracy being achieved in the reconstructed orbits (see section 4) implies residual delay errors of 50 ns with rates of change of 2×10^{-11}; the latter gives a residual fringe rate of 33 mHz at an observing frequency of 5.0 GHz. For each of the correlators being used with VSOP, table 3 gives the range of residual delay and fringe rate that can be accommodated. It can be seen that the accuracy being achieved is well within these ranges. This is fortunate because, although larger residuals could be accommodated, doing so would result in enormous output data sets, particularly for spectral line observations in which many frequency points per channel are desired.

The second set of information required is a series of time corrections produced by each tracking station. Timing information is conveyed to the correlator by embedding time labels in the recorded data, effectively labeling every data sample with a 'tape time.' All known errors are removed by adding the time correction series to the tape time.

7. Data Processing

The output of the correlator is the complex visibility function for each interferometer baseline as a function of residual delay and delay rate (e.g., Thompson et al. 1986). After correlation, AIPS (the Astronomical Image Processing System) is used to search for the peaks in this visibility function, the interference 'fringes' (Diamond 1995). *A priori* knowledge of the fringe location in delay/delay-rate space reduces the number of grid cells that must be considered as possible locations of the real signal, thereby reducing the signal-to-noise ratio required for detection. For space VLBI, the AIPS has been upgraded to allow the use of special techniques for the detection of fringes to the spacecraft, involving varying amounts of combining ground telescope data to give a higher signal-to-noise on baselines to the spacecraft.

It is desirable to integrate the data for long periods of time in order to improve the signal-to-noise ratio for detection, but the maximum integration time is limited by unmodeled phase variations in the link to HALCA. Measurements made from correlations of VSOP data show that coherence of greater than 90% is generally maintained for greater than 5 min at 1.6 and 5 GHz. Without the time corrections to the data from the tracking stations, the limit would be $\sim$ 30 s, preventing the detection of many weaker sources on baselines to HALCA.

The imaging techniques for VSOP data are very similar to those used for ground-based VLBI. Both AIPS (Diamond 1995) and the Difmap package (Shepherd 1997) have been upgraded for Space VLBI data. In imaging VSOP data, it is important to choose an appropriate visibility weighting scheme used when Fourier-transforming the visibility data to the image plane, since HALCA is a less sensitive antenna than a typical ground VLBI antenna. Consequently the r.m.s. noise level (σ) on space-baseline visibilities is higher than that on ground-only visibilities. Thus, the optimum point-source detection weighting scheme, called natural weighting, in which each visibility is weighted by σ^{-2} is inappropriate for imaging VSOP data since under this scheme the resolution of the VSOP image is almost the same as that of a ground-only image. Uniform weighting, where each visibility is weighted by the inverse density of (u, v)-points, is a more appropriate scheme for imaging VSOP data and provides about a factor of three increase in the linear resolution in VSOP images compared to ground-only images (Ulvestad 1999; Murphy et al. 2000a). However, this weighting scheme has some drawbacks in that the point-spread function has higher side-lobe levels and the r.m.s. noise level in the image is higher than that obtained when natural weighting is used. A hybrid of uniform and nat-

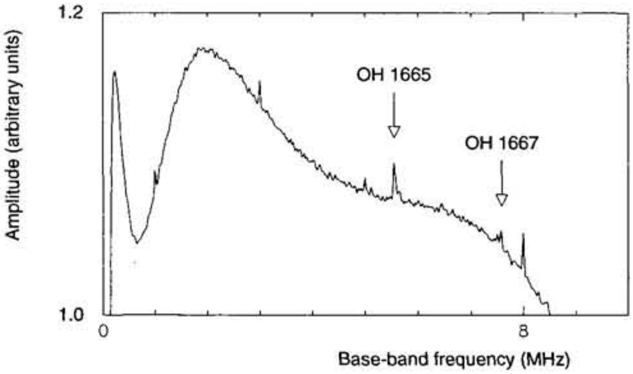

Fig. 3. HALCA's auto-correlation spectrum for a portion of one of the two 16 MHz channels from observations of W 49N on 1997 March 24. The base-band frequency for this channel is 1660 MHz and the autocorrelation used 1024 points per channel. The (rest frame) 1665.402 MHz and 1667.359 MHz OH lines can be clearly seen, both showing some structure. The DC offset (the spike near 0 MHz) is introduced by the Image Rejection Mixer on the satellite. Peaks at 1, 3, 5, and 8 MHz are spurious features that appear in autocorrelation spectra, but which do not cross-correlate strongly.

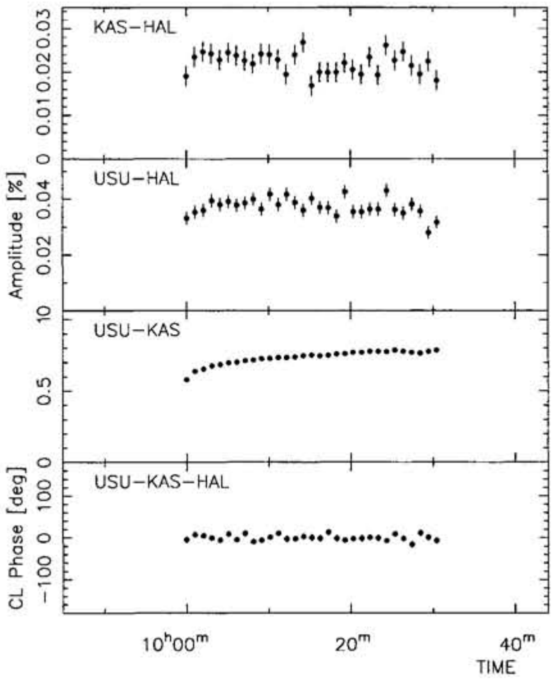

Fig. 4. Correlated amplitude (arbitrary units) and closure phase for an observation with HALCA (HAL), the Usuda 64 m telescope (USU), and the Kashima 34 m telescope (KAS) correlated at the Mitaka correlator. The closure phase for the triangle formed by the three telescopes is plotted in the bottom panel, with the phases clustering around zero, as expected for a compact source.

ural weighting is commonly used for imaging VSOP data as a trade-off between the two schemes. In AIPS this is achieved by using the parameter ROBUST in the IMAGR imaging task (Briggs et al. 1999) while in Difmap a similar result can be achieved by choosing suitable values of `bin_size` and `error_power` for the uvweight command. When making VSOP images one also needs to be aware of the usually large holes in (u, v)-plane (e.g., Murphy et al. 2000b; Okayasu et al. 2000) which are caused by the apogee height of the VSOP orbit exceeding an Earth diameter and which can also have a significant impact on the fidelity of VSOP images.

8. In-Orbit Checkout

The In-Orbit Checkout phase of the mission entailed a thorough testing of all the elements of the VSOP system described in the previous sections. The first astronomical pointing tests of HALCA were made of the OH maser source W 49N on 1997 March 24. HALCA's autocorrelation spectrum, showing the presence of the 1665.402 MHz and 1667.359 MHz maser lines, is shown in figure 3.

Observations with HALCA and the Usuda 64 m telescope of PKS 1519−273 at 1.6 GHz on 1997 May 7 resulted in 'first fringes' being detected on a baseline to the satellite at the Mitaka correlator on 1997 May 13. An observation with HALCA, the Usuda 64 m and the Kashima 34 m on 1997 May 13 of PKS 1504−166 enabled the closure phase to be determined. As shown in figure 4, the closure phase values are all close to zero, as expected for a point-like source.

These and other In-Orbit Checkout observations enabled the testing and debugging of the satellite, tracking stations, and correlators, and produced the first images ever produced by a space VLBI satellite and the accompanying ground resources. From 1997 July the number of In-Orbit Checkout observations was reduced and scientific observations started to be scheduled.

9. Observations

Before launch, the mission lifetime was expected to be 5 years, with cosmic-ray degradation of the solar panels providing the main limitation on the lifetime. After three years in orbit it is clear that the solar panel degradation is not as severe as had been anticipated, and that sufficient power will be available for over two more years of operation (Murata et al. 2000). The mission lifetime may, instead, be determined by other factors: only a small amount of hydrazine RCS fuel remains, and one reaction wheel has been taken out of operation.

To date, excluding periods where observing has been stopped, approximately 55% of the time has been used for maneuvers, calibration, maintenance, and testing of the satellite systems. About 30% of HALCA's in-orbit time is used for observing projects selected by international peer-review from open proposals submitted by the astronomical community in response to Announcements of Opportunity. This part of the mission's scientific programme constitutes the General Observing Time (GOT). The final 15% of the in-orbit time is devoted to a mission-led systematic survey of active galactic nuclei: the VSOP Survey Program (Hirabayashi et al. 2000). Survey observations are in general of shorter duration and made with fewer telescopes than the GOT observations. Nevertheless, the Survey will provide a large complete sample of homogeneous data on sub-milli-arcsecond radio structures, which is essential for studying cosmology and statistics of AGN, planning future VLBI observations, and for designing future Space VLBI missions.

10. Scientific Highlights

Most VSOP observations are made of extragalactic radio sources to study the compact cores and the milli-arcsecond scale jets, although observations of galactic hydroxyl masers and pulsars at 1.6 GHz have also be made. The longer baselines lengths, and gain in resolution, enabled by VSOP observations allow a range of unique scientific studies to be conducted, examples of which are given in this section.

Because the effects of "free–free" absorption are much larger at lower frequencies, the longest possible baselines are needed to provide adequate angular resolution; observing at higher frequencies to improve resolution does not help. The physical conditions in the inner parsec of accretion disks in galactic nuclei can be directly probed by imaging the absorption of background radio emission by ionized gas in the disk (e.g., Kameno et al. 2000; Jones et al. 2000)

VSOP observations allow "matched-resolution" spectral index maps of radio sources to be made. With ground-only arrays the resolution of spectral index maps always degrades to that of the lower frequency, however with space VLBI these losses are compensated for by the gains in baseline length. Spectral index maps allow wide-ranging studies of the parsec-scale radio emission to be made, including the presence or absence of synchrotron self-absorption in the core, and the evolution of the spectral index of jet components, with implications for the aging of the components and the shocks believed to generate them (e.g., Piner et al. 2000; Edwards et al. 2000).

The measurement of brightness temperature depends explicitly on the physical baseline length, and so the limits placed by space VLBI observations cannot be achieved by ground-based VLBI at other frequencies. The $\sim 10^{12}$ K inverse-Compton limit to the brightness temperature (Kellermann, Pauliny-Toth 1969) is a key method for constraining the doppler factor of the jet, which in turn provides information on the angle to the line of sight and the intrinsic jet speed. Both VSOP Survey Program observations and General Observing Time programs have found that many extragalactic radio sources have brightness temperatures in excess of the inverse-Compton limit (e.g., Bower, Backer 1998; Shen et al. 1999; Lovell et al. 2000; Preston et al. 2000; Frey et al. 2000).

HALCA only detects left circular polarized radiation. However, it is possible to record LCP with HALCA and both LCP and RCP at some ground radio telescopes, enabling polarization observations to be conducted (e.g., Kemball et al. 2000; Gabuzda 2000).

VSOP provides the only way to gain improved resolution for spectral line maser sources. VSOP observations have demonstrated that OH maser spots in the star-forming region OH 34.26+0.15 are only partially resolved, in contrast to expectations that interstellar scattering would result in a large degree of angular broadening at 1.6 GHz. The strongest peak has a brightness temperature in excess of 6×10^{12} K — exceeding the minimum value predicted by some models by an order of magnitude (Slysh et al. 2000). Results such as this have implications for our understanding of both maser physics and the interstellar medium.

Pulsars are strong radio sources at long wavelengths, so again, VSOP provides the only way to obtain improvements in resolution. VSOP observations of the Vela pulsar allow VSOP to become part of a "compound lens" and to use the magnification of the fluctuations in the interstellar medium. This technique dramatically increases the angular resolution achievable, and reveals that the pulsar's emission region is less than 500 km in extent (Gwinn et al. 2000). Similarly, VSOP observations of pulsars can in turn be used to determine the properties of the interstellar medium (Minter 2000).

11. Summary

The international cooperation and coordination required for VSOP observations make this one of the most complex space-science missions ever undertaken. The unique technical achievements of the mission to date have been the deployment in orbit of the 8 m antenna and tension-truss support structure, and the successful uplinking of the Doppler-corrected reference signal to HALCA and down-linking of the science data and determination of the necessary time corrections. The images of unprecedented resolution at 1.6 and 5 GHz resulting from the VSOP observations now being routinely undertaken are of fundamental importance to on-going efforts to understand the physical nature of the strongest, most compact radio sources in the Universe.

The VSOP Project is led by the Institute of Space and Astronautical Science, with significant contributions from the National Astronomical Observatory, the Jet Propulsion Laboratory, the U.S. National Radio Astronomy Observatory, the Canadian Dominion Radio Astrophysical Observatory, the Australia Telescope National Facility, the European VLBI Network, the Joint Institute for VLBI in Europe, and the Directors and staff of many of the world's radio observatories. In particular, the support and encouragement of Professors B. Burke, M. Oda and T. Nishimura in the early stages of the mission is gratefully acknowledged.

References

Benson J.M. 1995, in Very Long Baseline Interferometry and the VLBA, ed J.A. Zensus, P.J. Diamond, P.J. Napier, ASP Conf. Ser. 82, p117

Bower G.C., Backer D.C. 1998, ApJ 507, L117

Briggs D.S., Schwab F.R., Sramek R.A. 1999, in Synthesis Imaging in Radio Astronomy II, ed G.B. Taylor, C.L. Carilli, R.A. Perley, ASP Conf. Ser. 180, p127

Burke B.F. 1984, in VLBI and Compact Radio Sources, IAU Symp. 110, ed R. Fanti, K. Kellermann, G. Setti (Reidel, Dordrecht) p397

Carlson B.R., Dewdney P.E., Burgess T.A., Casorso R.V., Petrachenko W.T., Cannon W.H. 1999, PASP 111, 1025

Chikada Y., Kawaguchi N., Inoue M., Morimoto M., Kobayashi H., Mattori S., Nishimura T., Hirabayashi H. et al. 1991, in Frontiers of VLBI, ed H. Hirabayashi, M. Inoue, H. Kobayashi, (Universal Academy Press, Tokyo) p79

D'Addario L.R. 1991a, IEEE Trans. Instrum. Meas. 40, 584

D'Addario L.R. 1991b, NRAO OVLBI-ES Memo No. 12 (available from http://www.gb.nrao.edu/ovlbi)

D'Addario L.R. 1995, NRAO OVLBI-ES Memo No. 56 (available from http://www.gb.nrao.edu/ovlbi)

Diamond P.J. 1995, in Very Long Baseline Interferometry and the VLBA, ed J.A. Zensus, P.J. Diamond, P.J. Napier, ASP Conf. Ser. 82, 227

Edwards P.G., Giovannini G., Cotton W.D., Feretti L., Fujisawa K., Hirabayashi H., Lara L., Venturi T. 2000, PASJ 52, 1015

Frey S., Gurvits L.I., Altschuler D.R., Davis M.M., Perillat P., Salter C.J., Aller H.D., Aller M.F., Hirabayashi H. 2000, PASJ 52, 975

Gabuzda D.C. 2000, in Astrophysical Phenomena Revealed by Space VLBI, ed H. Hirabayashi, P.G. Edwards, D.W. Murphy (ISAS, Sagamihara) p121

Gwinn C.R., Reynolds J.E., Jauncey D.L., Tzioumis A.K., Carlson B., Dougherty S., Del Rizzo D., Hirabayashi H. et al. 2000, in Astrophysical Phenomena Revealed by Space VLBI, ed H. Hirabayashi, P.G. Edwards, D.W. Murphy (ISAS, Sagamihara) p117

Hirabayashi H., Fomalont E.B., Horiuchi S., Lovell J.E.J., Moellenbrock G.A., Inoue M., Burke B.F., Dewdney P.E. et al. 2000, PASJ 52, 997

Hirabayashi H., Hirosawa H., Kobayashi H., Murata Y., Edwards P.G., Fomalont E.B., Fujisawa K., Ichikawa T. et al. 1998, Science 281, 1825

Hirosawa H., Hirabayashi H. 1995, IEEE Aerospace and Electronic Systems Magazine 10, 17

Hirosawa H., Hirabayashi H. 1996, Space Technology 16, 161

Iguchi S., Kawaguchi N., Kameno S., Kobayahsi H., Kiuchi H. 2000, IEICE Trans. Comm. E83-B, 406

Jones D.L., Wehrle A.E., Piner B.G., Meier D.L. 2000, in Astrophysical Phenomena Revealed by Space VLBI, ed H. Hirabayashi, P.G. Edwards, D.W. Murphy (ISAS, Sagamihara) p71

Kameno S., Horiuchi S., Shen Z.-Q., Inoue M., Kobayashi H., Hirabayashi H., Murata Y. 2000, PASJ 52, 209

Kardashev N.S., Slysh V.I. 1988, in The Impact of VLBI on Astrophysics and Geophysics, IAU Symp. 129, ed M.J. Reid, J.M. Moran, (Reidel, Dordrecht) p433

Kellermann K.I., Pauliny-Toth I.I.K. 1969, ApJ 155, L71

Kemball A., Flatters C., Gabuzda D., Moellenbrock G., Edwards P., Fomalont E., Hirabayashi H., Horiuchi S. et al. 2000, PASJ 52, 1055

Kobayashi H., Shimoikura T., Omodaka T., Diamond P.J. 2000b, in Astrophysical Phenomena Revealed by Space VLBI, ed H. Hirabayashi, P.G. Edwards, D.W. Murphy (ISAS, Sagamihara) p109

Kobayashi H., Wajima K., Hirabayashi H., Murata Y., Kawaguchi N., Kameno S., Shibata K.M., Fujisawa K., Inoue M., Hirosawa H. 2000a, PASJ 52, 967

Levy G.S., Linfield R.P., Ulvestad J.S., Edwards C.D., Jordan J.F. Jr, Di Nardo S.J., Christensen C.S., Preston R.A. et al. 1986, Science 234, 187

Linfield R.P., Levy G.S., Edwards C.D., Ulvestad J.S., Ottenhoff C.H., Hirabayashi H., Morimoto M., Inoue M. et al. 1990, ApJ 358, 350

Linfield R.P., Levy G.S., Ulvestad J.S., Edwards C.D., DiNardo S.J., Stavert L.R., Ottenhoff C.H., Whitney A.R. et al. 1989, ApJ 336, 1105

Lovell J.E.J., Horiuchi S., Moellenbrock G., Hirabayashi H., Fomalont E., Dodson R., Dougherty S., Edwards P. et al. 2000, in Astrophysical Phenomena Revealed by Space VLBI, ed H. Hirabayashi, P.G. Edwards, D.W. Murphy (ISAS, Sagamihara) p183

Minter A. 2000, in Astrophysical Phenomena Revealed by Space VLBI, ed H. Hirabayashi, P.G. Edwards, D.W. Murphy (ISAS, Sagamihara) p113

Moellenbrock G.A., Kobayashi H., Murphy D.W. 2000, Adv. Sp. Res. 26, 613

Murata Y. and the HALCA Operation Group 2000, in Astrophysical Phenomena Revealed by Space VLBI, ed H. Hirabayashi, P.G. Edwards, D.W. Murphy (ISAS, Sagamihara) p9

Murphy D.W. and the VSOP International Team 2000a, Adv. Sp. Res. 26, 609

Murphy D.W., Tingay S.J., Preston R.A., Meier D.L., Guirado J.C., Polatidis A., Conway J.E., Hirabayashi H., Kobayashi H., Murata Y. 2000b, Adv. Sp. Res. 26, 665

Napier P.J., Bagri D.S., Clark B.G., Rogers A.E.E., Romney J.D., Thompson A.R. Walker R.C. 1994, Proc. IEEE 82, 658

Natori M., Takano T., Inoue T., Noda T. 1993, Design and Development of a Deployable Mesh Antenna for MUSES-B spacecraft (A93-1460) (AIAA, New York)

Natori M., Takano T., Ohnishi A., Miyoshi K., Inoue T., Tabata M., Kondo K. 1998, In-Orbit Deployment of a High Precision Mesh Antenna System for Space VLBI Mission (A98-1837) (AIAA, New York)

Ninomiya K., Hashimoto T., Kurii T., Ogura N. 1991 Proc. 1st ESA Int. Conf. Spacecraft Guidance, Navigation and Control Systems, ESA SP-323, p461

Okayasu R., Moellenbrock G., Ishizuki S., Kobayashi H., Murata Y., Edwards P., Hirabayashi H., Miyaji T. et al. 2000, Adv. Space Res. 26, 681

Pilbratt G. 1991, in Radio Interferometry: Theory, Techniques, and Applications, ed T.J. Cornwell, R.A. Perley, ASP Conf. Ser. 19, p102

Piner B.G., Edwards P.G., Wehrle A.E., Hirabayashi H., Lovell J.E.J., Unwin S.C. 2000, ApJ in press

Porcas R.W., Rioja M.J., Machalski J., Hirabayashi H. 2000, in Astrophysical Phenomena Revealed by Space VLBI, ed H. Hirabayashi, P.G. Edwards, D.W. Murphy (ISAS, Sagamihara) p245

Preston R.A., Lister M.L., Tingay S.J., Piner B.G., Murphy D.W., Meier D.L., Pearson T.J., Readhead A.C.S. et al. 2000, in Astrophysical Phenomena Revealed by Space VLBI, ed H. Hirabayashi, P.G. Edwards, D.W. Murphy (ISAS, Sagamihara) p199

Rogers A.E.E. 1995, in Very Long Baseline Interferometry and the VLBA, ed J.A. Zensus, P.J. Diamond, P.J. Napier, ASP Conf. Ser. 82, p93

Schilizzi R.T. 1988, in The Impact of VLBI on Astrophysics and Geophysics, IAU Symp. 129, ed M.J. Reid, J.M. Moran, (Reidel, Dordrecht) p441

Schilizzi R.T. 1995, Radio Science Bulletin 274, 14

Shen Z.-Q., Edwards P.G., Lovell J.E.J., Fujisawa K., Kameno S., Inoue M. 1999, PASJ 51, 513

Shepherd M.C. 1997, in Astronomical Data Analysis Software and Systems VI, ed G. Hunt, H.E. Payne, ASP Conf. Ser. 125, p77

Slysh V.I., Voronkov M.A., Migenes V., Shibata K.M., Umemoto T., Altunin V.I., Val'tts I.E., Kanevsky B.Z. et al. 2000, MNRAS in press

Suzuki K., Kawaguchi N., Kasuga T. 2000, in Astrophysical Phenomena Revealed by Space VLBI, ed H. Hirabayashi, P.G. Edwards, D.W. Murphy (ISAS, Sagamihara) p309

Thompson A.R., Moran J.M., Swenson G.W. Jr 1986, Interferometry and Synthesis in Radio Astronomy (Wiley, New York)

Tzioumis A. 1994, in VLBI Technology: Progress and Future Observational Possibilities, ed T. Sasao, S. Manabe, O. Kameya, M. Inoue (Terra Scientific, Tokyo) p211

Ulvestad J.S. 1999, in Synthesis Imaging in Radio Astronomy II, ed G.B. Taylor, C.L. Carilli, R.A. Perley, ASP Conf. Ser. 180, p513

Whitney A.R. 1999, New Astron. Rev. 43, 527

Wietfeldt R.D., Baer D., Cannon W.H., Feil G., Jakovina R., Leone P., Newby P., Tan H. 1996, IEEE Trans. Instrum. Meas. 45, 923

You T.-H., Ellis J., Mottinger N. 1998, in Spaceflight Dynamics 1998, ed T.H. Stengle, Adv. Astronautical Sci. 100, p873

Zensus J.A. 1997, ARA&A 35, 607